Journal of Engineering and Development, Vol. 11, No. 3, December (2007) ISSN 1813-7822

Error Correction Code in Optical Fiber

Dr. Mohammed Abdul-Alwahab
Laser & Optoelectronic Engineering Department
Technology University, Baghdad, Iraq

Asst. Lect. Sabah Abdul-Hassan Gitaffa
Electrical & Electronic Engineering Department
Technology University, Baghdad, Iraq

Eng. Raidh Adnan Kadhim
Technical Education Department
Technology University, Baghdad, Iraq

Abstract

Error correction codes have been successfully implemented in wire-line and wireless communication to offer error-free transmission with high spectral efficiency. The drive for increased transmission capacity in fiber-optic links has drawn the attention of coding experts to implement forward error correction (FEC) for optical communication systems in the recent past.

Particularly, the ITU-T G.975 recommended Reed-Solomon RS (255, 239) code, is now commonly used in most long-haul optical communication systems. It was shown that the code offers a net coding gain of around 4.3 dB for an output bit-error rate of 10-8 after correction. The Monte-Carlo simulation and theoretical performance analysis for the RS (255,239) code with 6.7% redundancy were presented for a completely random distribution of errors over an additive white Gaussian noise (AWGN) channel with BPSK signaling and hard decision decoding.

In addition, net coding gain comparison was done between the ITU-T G.975 standard and that offered by the RS (255, 247) and RS (255, 223) codes with 3.2% and 14.3% redundancy respectively.

الخلاصـــــة

*في الاتصالات السلكيه ولاسلكيه استخدام مرمز تصحيح الاخطاء الحاصله في عملية النقل وبكفائه طيف عاليه وخاليه من الاخطاء. ان الالياف البصريه تؤمن سعة نقل معلومات عاليه ولهذا تم التركيز على خبرة الترميز وتطبيقاتها في عملية تصحيح الاخطاء الاماميه (**FEC**).*

*ان مؤسسة (**ITU-T G,975**) توصي باستخدام ترميز نوع **Reed-Solomon RS (255,239)** في الاتصالات البصريه للمسافات البعيده لانه يؤمن ربح بالترميز مقداره **4.3db** وذلك من خلال التمثيل والتحليل النظري لهذا الترميز في القنوات ذات الترميز العشوائي للأخطاء والمضاف اليها ضوضاء البيضاء (**Gaussian noise**).*

*مع نوع من التحميل الاشاره (**BPSK**) وباستخدام فك المرمز صعب اضافة الى الربح الذي يحتويه هذا النوع من المرمز وباستخدام طريقه **RS (255-247)** و **RS (255-223)** تكون الإضافات للمرمز هي **3.2%** إلى**14.3** وعلى التوالي.*

1. Introduction

The noisy channel-coding theorem states that, the basic limitation that noise causes in a communication channel is not on the reliability of communication, but on the speed of communication [1,2]. The capacity of an additive white Gaussian noise (AWGN) channel is given by:

$$\mathbf{C = W\log(1+\tfrac{P}{N_0W})bits/sec} \quad \text{.. (1)}$$

where:

W: channel bandwidth in Hz.
P: signal power in watts
No: noise power spectral density in watts/Hz.

Channel capacity depends on two parameters namely, the signal power P and the channel bandwidth W. Increase in channel capacity as a function of power is logarithmic [3]. By increasing the channel bandwidth infinitely, we obtain:

$$\mathbf{\lim_{W\to\infty} C = 1.44\frac{P}{N_0}} \quad \text{... (2)}$$

Equation (2) means that channel capacity cannot be increased to any desired value by increasing W thus imposing a fundamental limitation on the maximum achievable channel capacity. Shannon [1,2], stated that there exist error control codes such that information can be transmitted across the channel at the transmission rate R below the channel capacity C with error probability close to zero. Thus, error-correction (control) coding (ECC), essentially a signal processing technique, in which controlled redundancy is added to the transmitted symbols to improve the reliability of communication over noisy channels can achieve transmission rate R close to the channel capacity C. The channel bandwidth of an optical communication system is larger (~100 THz) by a factor of nearly 10,000 times than that of microwave systems (~10 GHz). However, the channel capacity is not necessarily increased by the same factor because of the fundamental limitation stated above. The channel capacity given by (1) is the theoretical upper limit for a given optical fiber and depends upon the type of fiber. The present semiconductor and high speed optics technology is also a limitation to achieve excessively high data rates to take complete advantage of the enormous bandwidth offered by the fiber cable. Current light wave systems using single-mode fibers operate below the theoretical channel capacity, with bit rates 10 Gbits/s and above.

2. Distance-Capacity Metric

Just as speed-power product is a popular measure for gauging IC performance, distance capacity product provides a useful baseline for comparing optical communication systems. It is important to understand the channel impairments that limit the practically feasible transmission rates. However, increase in transmission rates can be achieved through multiplexing of multiple channels over the same fiber by the use of Time Division (TDM) or Frequency Division Multiplexing (FDM) techniques. In the optical domain, FDM is referred as Wavelength Division Multiplexing (WDM). TDM increases the data rate of the system by sending more data in the same amount of time by allocating less time for each individual bit that is sent. But we have to pay a price for it not only in terms of increased component complexity associated with the transmission, but also the properties of the fiber and the signal degrade at higher data rates. TDM is not considered any further, while treatment to WDM is given where necessary. By using, WDM different wavelengths (frequencies)1 are used to transmit independent channels of information. Again, there are limiting factors to WDM transmission that involve the degradation of signal transmission quality. The distance capacity metric is a function of two parameters, viz., the number of wavelengths that can be transmitted via WDM and the rate at which data is transmitted on these wavelengths.

3. Optical Communication System Model

The optical communication system model is depicted in **Fig.(1)**. The information source generates a sequence of binary bits. For the Reed-Solomon encoder these binary bits are grouped to form q-ary symbols from GF ($q=2^m$). These symbols (bits) in turn are grouped into blocks of k symbols denoted by $u = (u_1, u_2,\ldots, u_k)$ the message block. The channel encoder adds controlled amount of redundant symbols to each of the k symbol message blocks to form code word blocks of n symbols denoted by $v = (v_1, v_2,\ldots, v_n)$.

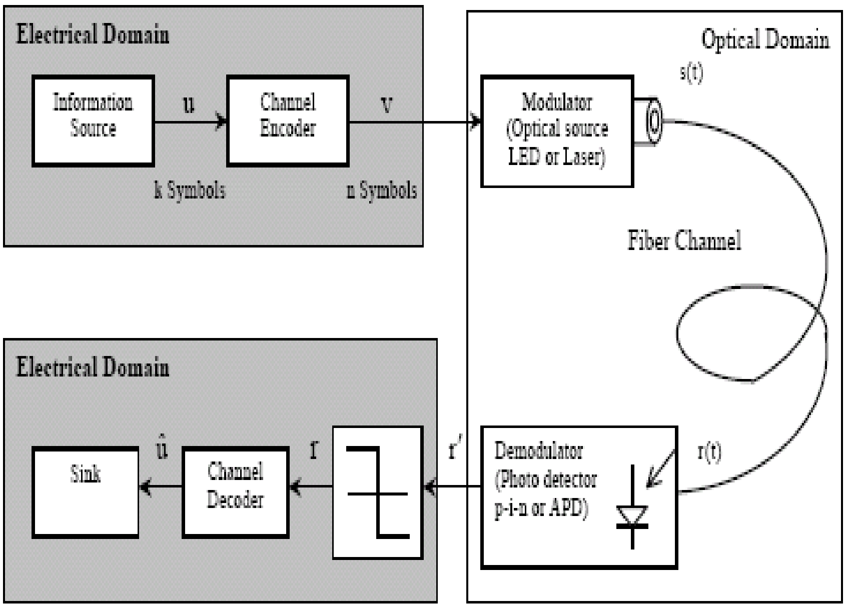

Figure (1) Optical communication system models

In this paper, we have used a digital transmission scheme in which an electrical bit stream modulates the intensity of the optical carrier (modulated signal). The modulated signal is detected directly by a photo detector to convert it to the original digital (modulating) signal in the electrical domain. It is referred to as Intensity Modulation with Direct Detection (IM/DD) or On-Off Keying (OOK) or Amplitude Shift Keying (ASK). When the RS encoder is used, the q-ary symbols have to be translated into a sequence of $\log_2(q)$ binary bits before driving the optical source. The output of the modulator is an optical pulse of duration T for bit 1 and no pulse for bit 0. Thus a signal waveform $S_i(t)$ of duration T is transmitted over the fiber optic channel such that:

$$\begin{aligned} \mathbf{S_i(t) = A} \quad & \mathbf{;i = 1} \\ \mathbf{= 0} \quad & \mathbf{;i = 0} \end{aligned} \quad \text{.......... (3)}$$

where:

A: is the amplitude of the transmitted optical pulse

A mathematical model for the optical channel is the AWGN channel which models Gaussian (thermal) noise present at the receiver's front-end electronic circuitry. In the model, a Gaussian random noise process n (t) is added to the transmitted signal waveforms (t) [4]. Which is a vector representation where (v) represents the transmitted code word, e represents the white noise process and the corrupted received word is represented as r′. At the receiver, the demodulator is a photo detector (p-i-n or APD), which converts the received optical signal r(t) into electrical current I (t). The vector r′ in the model is obtained as the output of the demodulator. The vector r′ contains sufficient statistics for the detection of the transmitted Symbols [4]. A sequence of vector r′ is then fed to the decoder, which attempts to reconstruct the original message block uˆ, using the redundant symbols. In many situations, the vector r′ is passed through the threshold detector, which provides the decoder a vector r with only binary zeros and ones. In such a case the decoder is said to perform hard decision decoding and the resulting channel consisting of the modulator, AWGN channel, demodulator and detector is called the Binary Symmetric Channel [4]. The AWGN and BSC channel models are used throughout the report for our analysis.

4. Maximum Likelihood Decoding

Assuming that the decoder has received a vector r′, which is unquantized the optimum decoder that minimizes the probability of error will then select the vector vˆ = vj iff [4].

$$\mathbf{Pr(V_j \backslash r') > Pr(V_i \backslash r')} \quad \text{.......... (4)}$$

where:

$\forall i \neq j$

This is known as the maximum a posteriori probability (MAP) criterion, using Bayes rule.

$$\mathbf{Pr(V_i \backslash r') = \frac{Pr(V_i)p(r' \backslash V = V_i)}{p(r')}} \quad \ldots\ldots (5)$$

where:

$\Pr(V_i \backslash r')$ *for* $i = 1,2,..., q^K$ *: are the posterior probabilities*

$p(r' \backslash V = V_i)$ *: is the conditional pdf of r′ given*

V_i: is transmitted and called the likelihood function.

$Pr(V_i)$: is the a priori probability of the i^{th} vector being transmitted and,

$$\mathbf{P(r') = \sum_{i=1}^{q^K} P(r' \backslash V_i) Pr(V_i)} \quad \ldots\ldots (6)$$

Computation of the posterior probabilities $\mathbf{Pr(V_i \backslash r')}$ is simplified when the q^k vectors are equiprobable and p(r′)is independent of the transmitted vector. The decision rule based on finding the vector that maximizes $\mathbf{Pr(V_i \backslash r')}$ is equivalent to finding the signal that maximizes $\mathbf{p(r' \backslash V = V_i)}$. Thus the MAP criterion simplifies to the maximum-likelihood (ML) criterion and the optimum decoder then sets $\mathbf{\hat{V} = V_j}$ iff

$$\mathbf{P(r' \backslash V = V_j) > P(r' \backslash V = V_i)} \quad \ldots\ldots (7)$$

where:

$\forall i \neq j$

For the AWGN channel the likelihood function is given as:

$$\mathbf{P(r' \backslash V = V_i) = P(r' - V_i \backslash V = V_i) = \frac{1}{\sqrt{2\prod\sigma^2}} e^{-|r'-V_i|^2 / 2\sigma^2}} \quad \ldots\ldots (8)$$

Taking the natural logarithm, we have:

$$\mathbf{InP(r' - V_i \backslash V = V_i) = -\frac{1}{2} In(2\prod\sigma^2) - \frac{1}{2\sigma^2} |r' - V_i|^2} \quad \ldots\ldots (9)$$

Consequently the optimal ML decoder will set $\hat{V} = V_j$ iff

$$\mathbf{|r' - V_j|^2 < |r' - V_i|^2 \quad ; \forall i \neq j} \quad \ldots\ldots (10)$$

$$\left|\mathbf{r'} - \mathbf{V_i}\right|^2 = \sum_{l=1}^{n} (\mathbf{r}_l - \mathbf{V}_{il})^2 \quad ;\forall \mathbf{i} = 1,2,\ldots \mathbf{q}^k \quad \ldots\ldots\ldots\ldots\ldots\ldots\ldots\ldots \mathbf{(11)}$$

is the squared Euclidean distance. Hence, for the AWGN channel, the decision rule based on ML criterion simplifies to finding the vector V_i that is closest to the received vector r′ in the Euclidean distance sense. If hard decision is made on r′ prior to decoding by means of a threshold detector, then the BSC replaces the AWGN and the ML decoder will select $\hat{V} = V_j$ iff.

$$\mathbf{P(r \setminus V = V_j) = P(r \setminus V = V_i)} \quad ;\forall \mathbf{i \neq j} \quad \ldots\ldots\ldots\ldots\ldots\ldots\ldots\ldots \mathbf{(12)}$$

where:

r = (r_1, r_2,…, r_n)and

$r_1 \in \{0,1\}$; $\forall 1=1,2,\ldots,n$.

The BSC flips a binary '0' to a binary '1'with probability p called the transition probability. The number of components in which r and V_i differ is called the Hamming distance and the ML decoding criterion for hard decision decoding simplifies to finding V_i that is closest to the received vector r in the Hamming distance sense.

5. Theoretical and Simulated Results

5-1 Performance of RS Codes

The different RS code parameters are presented in **Table (1)**. From **Table (1)** we observe as the code rate decreases the redundancy in the code, the minimum distance of the code and the asymptotic coding gain increases. The code rate and redundancy are inversely proportional to each other. Since it is difficult to calculate the WEF of the candidate RS codes, we have used the approximation given by (13, 14 and 15) to compute the analytical output BER.

$$\mathbf{P_{sc} = 1 - (1 - P)^{m/b} ; b = 1} \quad \ldots\ldots\ldots\ldots\ldots\ldots\ldots\ldots \mathbf{(13)}$$

where:

$P = Q\left(\sqrt{\dfrac{2 * R_c * E_b}{N_0}}\right)$: R_c is the code rate of the code.

Table (1) RS code parameters

Candidate RS (n, k) Codes	Code Rate (k/n)	Redundancy (n-k)/k (%)	d_{min} (2*t+1)	G_a (dB) Asymptotic
RS (255, 247)	0.9686	3.24	9	9.4
RS (255, 239)	0.9372	6.69	17	12.02
RS (255, 223)	0.8745	14.35	33	14.6

The value of P gives the information BER at the input of the decoder. The probability of uncorrectable word error [5] is given by:

$$P_u(E) \approx \sum_{i=t+1}^{n} \frac{i}{n} \binom{n}{i} P_{sc}^{\ i} (1-P_{sc})^{n-i} ; n = q^m - 1 \ldots\ldots\ldots\ldots\ldots\ldots\ldots\ldots\ldots\ldots\ldots\ldots \quad (14)$$

The information BER at the output of the decoder [5] is given by:

$$P_{b(output)} \approx 1 - (1 - P_n(E))^{1/m} \ \ldots\ldots\ldots\ldots\ldots\ldots\ldots\ldots\ldots\ldots\ldots\ldots\ldots\ldots \quad (15)$$

We extend the approximation for the RS codes presented in **Table (1)** to compute the approximate BER analytically. The analytical results for the candidate RS codes are presented in **Fig.(2)**. The Monte-Carlo simulations were performed piece-wise for an output BER of $\leq 10^{-8}$ for the candidate RS codes. The simulated results presented in **Fig.(3)** are confirmed with the analytical results in **Fig.(2)**. The simulated curves presented in **Fig.(3)** are extrapolated for an output BER of $\leq 10^{-12}$. These extrapolated curves are presented in **Fig.(4)**. Net electrical coding gain (NECG) is commonly used to quantify FEC performance and indicates an improvement in the SNR or Q factor at the receiver due to FEC.

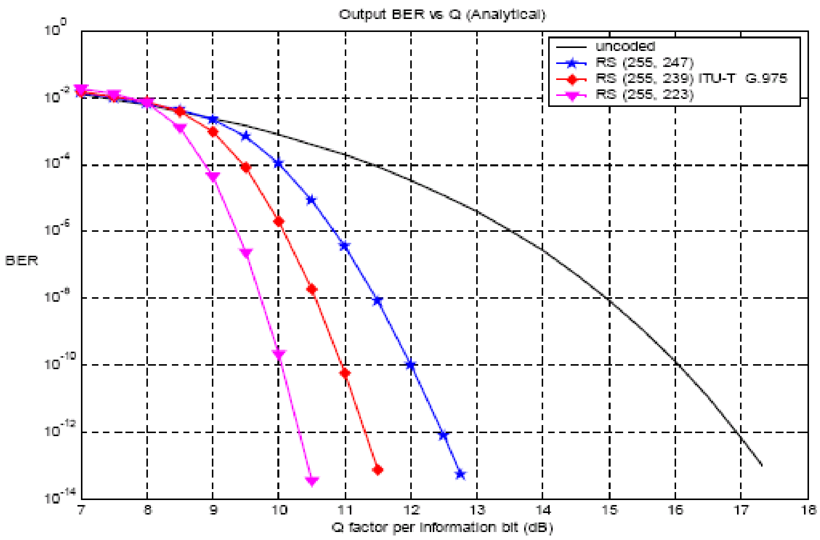

Figure (2) Theoretical performance of the RS codes

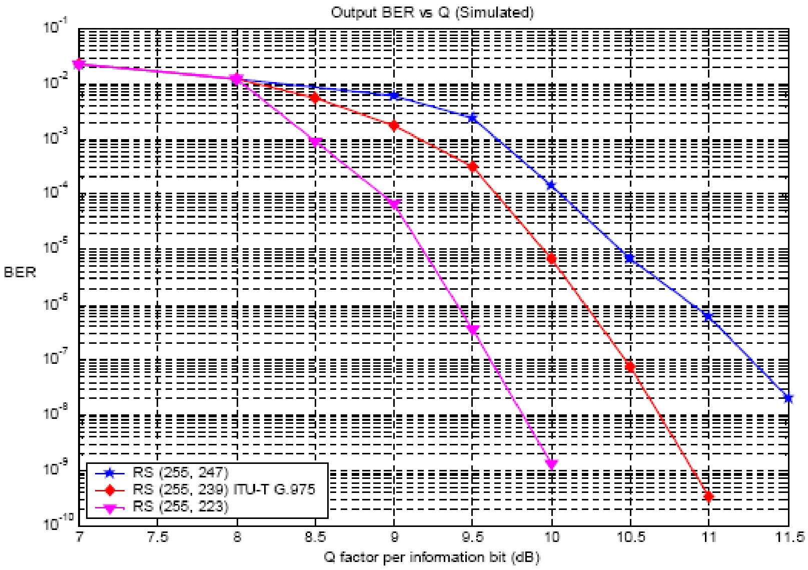

Figure (3) Simulated performance of the RS codes

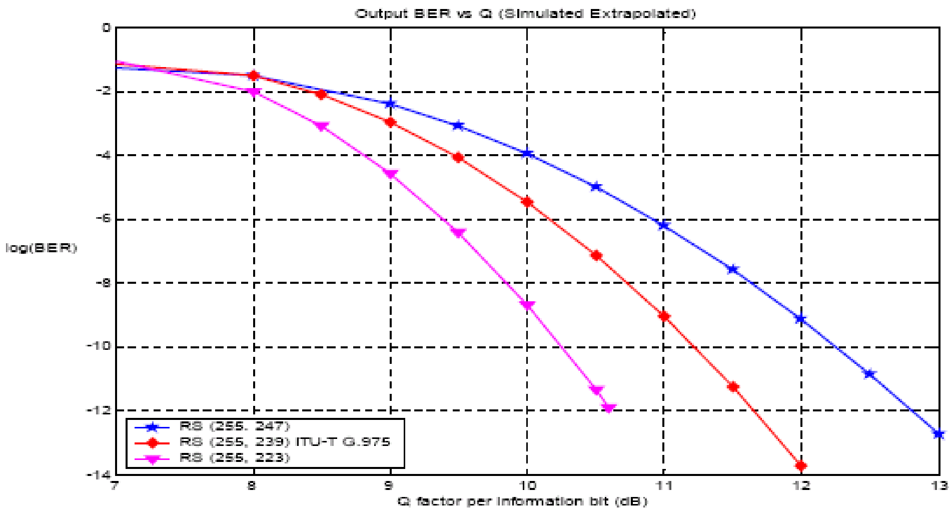

Figure (4) Simulated performance of the RS codes (Extrapolated to $\leq 10^{-12}$)

The comparison of the performance of the candidate RS codes in terms of coding gain is presented in **Table (2)**. The coding gain comparison of the candidate RS codes for an output BER of $\leq 10^{-8}$ is obtained from **Fig.(2)** and **Fig.(3)** whereas that for an output BER of $\leq 10^{-12}$ is obtained from **Fig.(2)** and **Fig.(4)**.

Table (2) Coding gain comparison of the RS codes at output BER of 10^{-8} and 10^{-12}

Candidate RS (n,k) Codes	Redundancy (n-k)/k (%)	NECG (dB) @ BER $\leq 10^{-8}$ (Theoretical)	NECG (dB) @ BER $\leq 10^{-8}$ (Simulated)	NECG (dB) @ BER $\leq 10^{-12}$ (Theoretical)	NECG (dB) @ BER $\leq 10^{-12}$ (Sim.Ext.⊥)
RS (255, 247)	3.24	3.5	3.37	4.46	4.2
RS (255, 239)	6.69	4.42	4.28	5.63	5.3
RS (255, 223)	14.35	5.25	5.15	6.62	6.33

It can be noticed from **Table (2)** the increased redundancy in the code pays in terms of NECG. The RS (255, 239) code with almost twice the redundancy compared to the RS (255, 247) code offers roughly more than 1dB additional coding gain. Approximately 2dB additional coding gain is offered by the RS (255, 223) code with almost 4.5 times more redundancy than the RS (255, 247) code. The theoretical curve for the ITU-T G.975 standard in **Fig.(2)** is confirmed with [5] while the simulated curve presented in **Fig.(3)** is confirmed with [6]. The simulated results for RS (255, 223) and RS (255, 247) are in coherence with [7] and [8] respectively.

The (theoretical and simulated) performances of the candidate RS codes in terms of output BER vs. input BER are depicted in **Figs.(5)** and **(6)** respectively. The output BER performance of the candidate codes at an input BER of 10^{-3} is presented in **Table (3)**. From **Table (3)** it can be observed that for a fixed value of input BER the output BER decreases as the redundancy in the code increases. For the ITU-T standard with almost twice the redundancy in the RS (255, 247) code the output BER is reduced approximately by a factor of 10^{-2}. The output BER (theoretical) of $5*10^{-15}$ for input BER of 10^{-4} for the ITU–T G.975 standard is confirmed with [5].

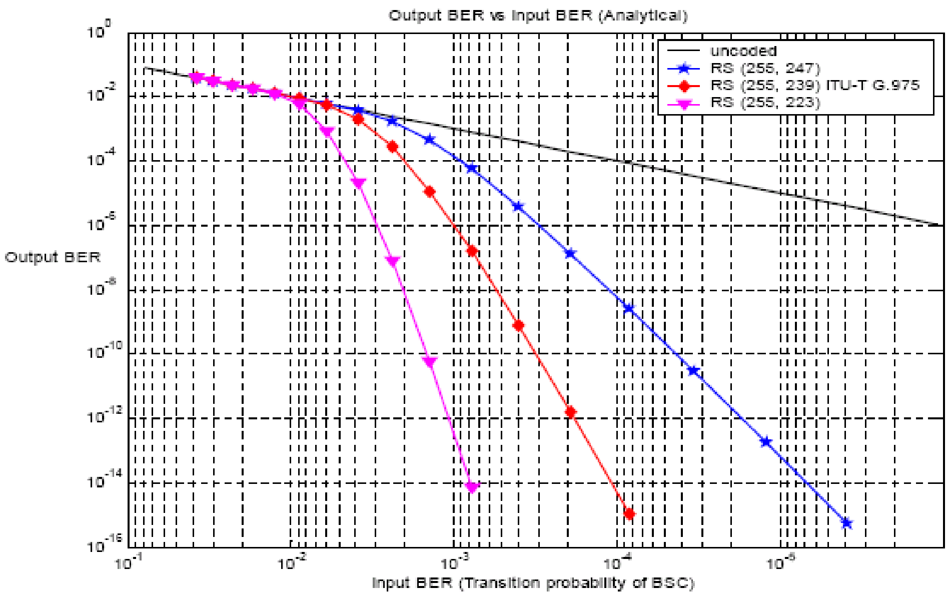

Figure (5) Theoretical output BER vs. input BER performance

Table (3) Output BER comparison of the RS codes at input BER of 10^{-3}

Candidate RS (n, k) Codes	Redundancy (n-k)/k (%)	Output BER (Theoretical)	Output BER (Simulated)
RS (255, 247)	3.24	$1*10^{-4}$	$1.5*10^{-4}$
RS (255, 239)	6.69	$9*10^{-7}$	$1*10^{-6}$
RS (255, 223)	14.35	$3*10^{-13}$	-

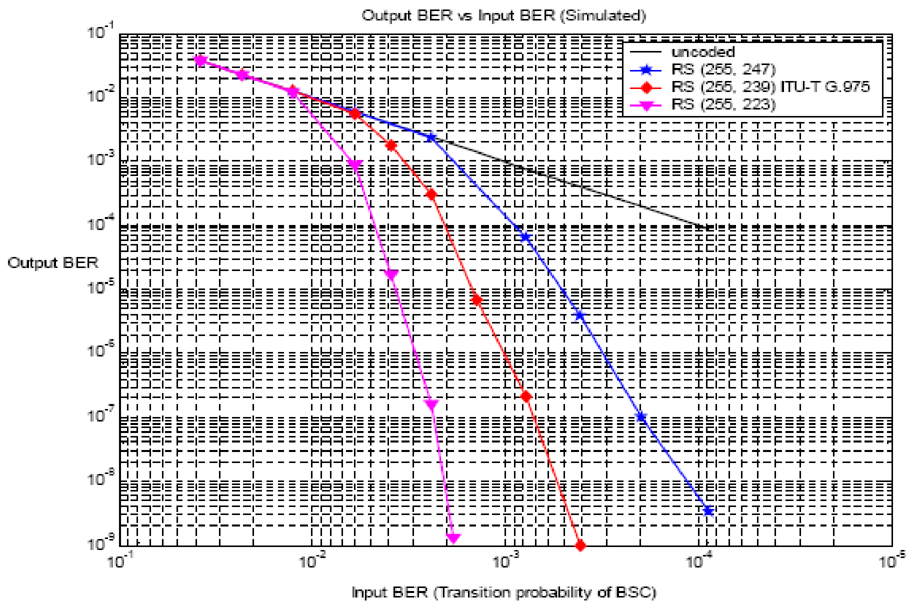

Figure (6) Simulated output BER vs. input BER performance

5-2 Remarks and Conclusion

The main objective of this paper project was to investigate the advantages and limitations of different FEC solutions regarding performance and feasible ways of implementation. The work presented in the report was more theoretical based on analytical and computer simulation results. The presented work could be further continued with a hardware implementation of a encoder/decoder in a fiber-optic transceiver. A scalable RS encoder/decoder operating at low data rate could be initially implemented with a FPGA for single channel as well as multichannel systems. Laboratory experiments at low data rate and variable span of fiber link could be conducted on the transceiver with FEC by introducing and varying the critical channel impairments. With positive outcome of these experiments, an ASIC implementation with parallel operations may be realized considering cost and power consumption. RS decoder designs and architectures implemented in VLSI circuits for the long RS codes are found in [9, 10, and 11]. Efficient implementation of finite-field arithmetic operations is presented in [12, 13, 14, and 15].

Optical networks have evolved significantly over the past few years, moving from data rates of 2.5 Gbits/s to 10 Gbits/s and looking forward to 40 Gbits/s and beyond. As the transmission speed increases on one hand, the transmission impairments also increase on the other. In many cases, the impairments increase in a nonlinear fashion, even though the transmission rates are increasing linearly. The same phenomenon is also true for WDM systems. Hence, FEC becomes vital in single channel as well as multi-channel WDM systems for delivering error free transmission between 10-100 Gbits/s for next generation optical systems.

6. References

1. C. E., Shannon, ***"A Mathematical Theory of Communication"***, Bell System Technical Journal, Vol. 27, July (1948a), pp. 379-423.

2. C. E., Shannon, ***"A Mathematical Theory of Communication"***, Bell System Technical Journal, Vol. 27, October (1948b), pp. 623-656.

3. J. G., Proakis, and M., Salehi, ***"Communication Engineering"***, 1st Edition, Upper Saddle River, NJ, Prentice Hall Inc, 1994.

4. J. M., Wozencraft, and I. M., Jacobs, ***"Principles of Communication Engineering"***, New York, John Wiley and Sons, 1965.

5. ITU-T G.975, ***"Forward Error Correction for Submarine Applications"***, October 2000.

6. O. A., Sab, ***"Concatenated Forward Error Correction for Long-Haul DWDM Optical Transmission Systems"***, Proceedings for ECOC, 1999.

7. O. A., Sab, and R., Pyndiah, ***"Performance of Reed-Solomon Block Turbo Code"***, Proceeding of IEEE GLOBECOM Conference, Vo1. 1/3, Nov. 1996, pp. 121-125.

8. K., Azadet, E., Haratsch, H., Kim, F., Saibi, J., Saumders, M., Shaffer, L., Song, and M. L., Yu, ***"DSP Techniques for Optical Transceivers"***, IEEE, 2001, pp. 281-287.

9. B., Green, and G., Drolet, ***"A Universal Reed-Solomon Decoder Chip"***, Proceedings of the 16th Bieunial Symposium on Communications, Kingston, Ontario, May 1992, pp. 327-330.

10. K., Seki, K., Mikami, M., Baba, N., Shinonhara, S., Suzuki, H., Tezuka, S., Uchino, N., Okada, Y., Kakinuma, and A., Katayama, ***"Single-chip 10.7 Gb/s FEC CODECLSI Using Time Multiplexed RS Decoder"***, IEE Custom Integrated Circuits Conference, 2001, pp. 289-292.

11. H., Tezuka, I., Matsuoka, T., Asahi, N., Arai, T., Suzaki, Y., Aoki, and K., Emura, ***"2.677 Gbit/s-Throughput Forward Error Correction LSI for Long-Haul Optical Transmission Systems"***, ECOC, September 1998, pp. 561-562.

12. ITU-T G.975, ***"A VLSI Architecture for a Low Complexity Rate Adaptive Reed-Solomon Encoder"***, Proceedings of the 16th Biennial Symposium on Communications, Kingston, Ontario, May 1992, pp. 331-334.

13. M. A., Hasan, and V. K., Bhargara, ***"Bit Serial Divider and Multiplier for GF (2m)"***, IEEE Transactions on Computers, Vo1. 41, August 1992, pp. 972-980.

14. J. L., Massey, and J. K., Omura, ***"Apparatus for Finite Field Computation"***, 1984, pp. 21-40.

15. J. L., Massey, and J. K., Omura, ***"A Systolic Reed-Solomon Encoder"***, IEEE Transactions on Information Theory, Vo1. IT-37, July 1991, pp. 1217-1220.